

# Precision Geolocation of Propagation Data Using GPS and Data Fusion

Anna E. Paulson  
Institute for Telecommunication Sciences  
Boulder, CO, USA  
apaulson@ntia.gov

**Abstract**—Geopositioning uncertainty degrades the usefulness of the data collected while conducting propagation measurements in the field. Researchers currently have access to highly detailed terrain, propagation, and locational data sets, but these data are useless if you don't know where you are in the world; this, in turn, hampers the development of propagation models. This paper describes a commercial off-the-shelf engineering solution being developed by the US Department of Commerce's Institute for Telecommunication Sciences that mitigates the problem of dynamic positioning in urban corridors and reduces our positioning uncertainty by as much as an order of magnitude in the horizontal plane.

**Keywords**—GPS, GNSS, SLAM, terrain clutter, geolocation, RF propagation

## I. INTRODUCTION

Beginning in 2016, the US Department of Commerce's Institute for Telecommunication Sciences (ITS), the research and development laboratory for the National Telecommunication and Information Administration, started taking steps to improve the geopositioning capability of its propagation measurement systems. Prior to this effort, ITS had been using small, surface-mount "hockey puck"-type global positioning system (GPS) antennas (single frequency, low gain, right-hand circularly-polarized, hemispherical antenna pattern) when collecting Radio Frequency (RF) propagation data during drive testing. Typically, these antennas would be connected directly to a vector spectrum analyzer to provide latitude, longitude, and time/date stamps for each collected data point.

The overall GPS solution used when drive testing, of which the small, surface mount antenna was one part, performed well with respect to time/date stamps, but the horizontal position estimate (lat/lon) was highly variable; height above ground estimates more so — positional uncertainty at the start of the project was as high as 5 m in outdoor areas with a generally unobstructed view of the sky (e.g. "blue sky" rural and suburban areas) and dramatically higher, as much as 40 m, in urban areas with an obstructed view of the sky (urban canyons).

However, given the nature of the RF signal under test — a continuous wave signal transmitted in the 1–3 GHz range — some positional error was acceptable and met our self-imposed requirement. This will be discussed in more detail in Section III, but the effective margin of error chosen for the position estimate is the first Fresnel zone — so long as we knew that we were capturing signals within the first Fresnel zone, positional uncertainty could be mitigated by ground truth, e.g., the drive test route was known in advance, the measurement team knew it

was traveling on a single lane on a road in a particular direction, the receive antenna was placed at a known, fixed height above the road on the drive test vehicle, etc.

ITS's precision geolocation system, described in detail in Section II, has evolved to include a sophisticated Global Navigation Satellite System (GNSS) receiver, several real-time streaming position correction sources, and additional position sensors. An investment in new equipment and time has borne fruit — to date, we have achieved a nearly 600 fold improvement in accuracy under static, "blue sky" conditions. These initial improvements were made possible by simply spending time with the equipment and identifying the optimal settings for each use case. This practice eventually led to a set of best practices [1].

The final challenge is to improve the positional accuracy under urban canyon conditions. This is a difficult problem because the GNSS receiver is susceptible to a strong multipath environment in urban canyons. A lesser, though still difficult, problem is the fact that GNSS antennas sometimes lose visibility to all satellites or cannot maintain the minimum number of satellite vehicles needed for a position fix in three dimensions. The solution to the urban canyon problem involves fusing GNSS data with data from other sensors to arrive at a final position guess that is both accurate (as close as possible to ground truth) and precise (repeated trials yield similar position results). We hope to deliver a cost-effective system and solution set that can be replicated by other commercial, governmental, and academic institutions.

## II. SYSTEM OVERVIEW

The precision geolocation system, seen below in Fig. 1, is, by design, a collection of commercial off-the-shelf (COTS) equipment. The components can be broadly characterized as signal sources, sensors, correction sources, and processing algorithms. A brief operational description of each major component in the system and a general signal flow are given below.

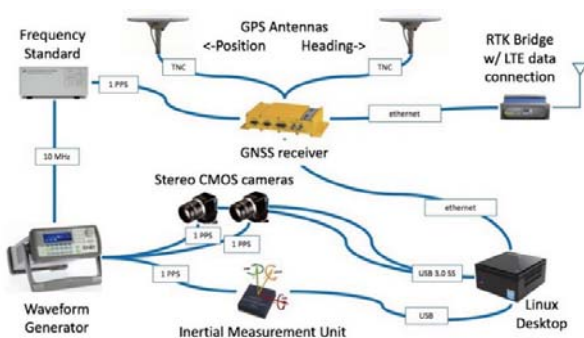


Fig. 1. A system-level diagram of ITS's precision geolocation system showing individual components and interfaces.

By far the most important of the sensors is the Trimble™ BX982 global navigation satellite system (GNSS) receiver. The receiver provides our baseline position estimate and is capable of processing both position and heading information from the major global positioning satellite constellations, e.g. GPS, GALILEO, GLONASS, BeiDou, etc. The receiver also provides a 1 Hz or pulse-per-second (PPS) reference signal via a 50 Ω Bayonet Neill–Concelman (BNC) connector, and outputs a wealth of GPS information in NMEA-0183 format via a 100 Mb/s Ethernet connector [2].<sup>1</sup>

The GNSS receiver can correct the position information it receives in several ways, e.g. through code-differential GPS (C-DGPS), Satellite-based Augmentation System (SBAS), and Real Time Kinematics (RTK). C-DGPS and SBAS are calculated in the receiver using the satellite signals themselves, while RTK can be delivered via satellite or the Internet. In the precision geolocation system, RTK corrections are delivered via satellite at the Trimble receiver through a proprietary, subscription-based service known as CenterPoint RTX™, and via an Ethernet connection from an Intuicom™ Wireless RTK Bridge with a cellular (4G LTE) data connection [3]. Specifically, the RTK bridge connects to a University Navstar Consortium (UNAVCO) Plate Boundary Observatory Networked Transport of RTCM via Internet Protocol (NTRIP) server [4]. The RTK bridge also provides a dedicated, wireless Internet connection for use in the field.

The GNSS receiver sends a one pulse per second signal via a coaxial cable terminated at both ends with a 50 Ω BNC connector to a Stanford Research Systems™ FS275 rubidium frequency standard. This signal is used to discipline the rubidium oscillator, which serves as our primary reference for time-based signaling. The rubidium frequency standard outputs a 10 MHz reference signal to an Agilent™ 33205A Function/Arbitrary Waveform Generator using the coaxial cable described above. The waveform generator, in turn, provides a set of two Ximea™ xiQ Universal Serial Bus 3.0 SuperSpeed (USB3.0 SS) Complementary Metal Oxide Semiconductor (CMOS) sensor digital cameras and a Gladiator Technologies LandMark01™ Inertial Measurement Unit (IMU) waveform generator with a 1 PPS signal. In the precision geolocation

system, we use the 1 PPS signal as a trigger source to capture a digital image from each camera (both of which are mounted facing the same direction, approximately six inches away from each other) simultaneously and as an external synchronization input for the IMU. Collecting data on a 1 PPS basis allows ample time to collect data points from all sensors and process them into a final positional guess.

Finally, a desktop computer running a 64-bit version of Ubuntu Linux is used for data collection, processing, and display while in the field. Data is collected from each sensor (GNSS, IMU, and cameras) and processed into a common format using MATLAB® scripts and Application Program Interface (API) commands supplied by the equipment vendor. In the case of the computer vision cameras, an open-source application called OpenCV is used in conjunction with the Ximea API to determine a set of landmarks in common between each camera's view. The desktop computer also performs some auxiliary functions such as accessing equipment web interfaces (Trimble and Intuicom), starting/stopping data collection via a MATLAB graphical user interface (GUI), and displaying final position estimates in Google Earth™.

### III. IMPLICATIONS OF POSITIONAL ERROR

This section describes a practical limit for errors in position estimates that occur during drive testing, namely the width of the first Fresnel zone. This baseline was chosen because it is a familiar concept in RF propagation measurements and happens to correspond to real-world drive test conditions, i.e. it's about the width of a large, urban street.

A graphical representation of a Fresnel zone is given in Fig. 2. A Fresnel zone calculation is normally included in a site survey's terrain profile, as obstructions that occur within the zone will lead to destructive interference at the receiving antenna and thus will degrade the signal, increase the amount of path loss, etc. [5] This zone, when constrained to two dimensions, is an ellipse described below in (1) ...

<sup>1</sup> Certain commercial equipment and materials are identified in this report to specify adequately the technical aspects of the reported results. In no case does such identification imply recommendation or endorsement by the

National Telecommunications and Information Administration, nor does it imply that the material or equipment identified is the best available for this purpose.

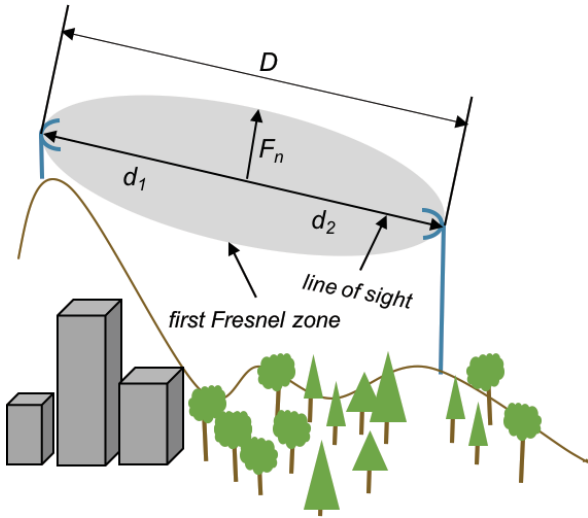


Fig. 2. An illustration of a typical line-of-sight radio link and terrain profile outline showing the parameters used in calculating the radius of the Fresnel zone ( $F_n$ ).

$$F_n = \sqrt{\frac{nd_1d_2}{fD}} \quad (1)$$

...where  $F_n$  is  $n$ th Fresnel zone radius in meters,  $D$  is the total path distance  $D = d_1 + d_2$  or line-of-sight path between the transmitter and receiver in kilometers,  $d_1$  and  $d_2$  are the distance from the transmitter and receiver to some point along the edge of the ellipse, and  $f$  is the frequency of the transmitted signal in gigahertz. This equation can be practically simplified for the first Fresnel zone ( $n=1$ ) radius maxima, where  $d_1 = d_2$ , [5] to

$$F_n = 17.3 \sqrt{\frac{D}{4f}} \quad (2)$$

A typical frequency for the types of drive testing ITS performs would be in the Advanced Wireless Service-3 Block (AWS-3) [2], e.g. 1.7 GHz, with a total transmit path distance of approximately 3 km, thus yielding a first Fresnel zone radius of...

$$F_n = 17.3 \sqrt{\frac{3 \text{ [km]}}{4 \cdot 1.7 \text{ [GHz]}}} \approx 11.5 \text{ m} \quad (3)$$

The distance calculated above in (3) is the baseline for positional drift; meaning, positional drift outside of 11.5 m, or approximately the width of a four-lane road in the United States [7], would put us outside of the first Fresnel zone.

Naturally, obstructions within the first Fresnel zone would be avoided if the researcher is solely interested in characterizing the propagation characteristics of a radio channel. ITS's precision geolocation system was designed to provide location data when measuring clutter, or "excess loss due to attenuation from buildings and vegetation, above either free-space path

losses or terrain attenuation." [8] So, in this specific case, buildings and vegetation are extant in the first Fresnel zone for much of the drive test, and propagation losses due to clutter were extracted from the data

The limit given above in (3) is being met with the current iteration of the precision geolocation system, even under dynamic, urban canyon conditions, as will be shown in the following section. Given that, why is it necessary to improve our positioning capability? ITS is also preparing to conduct field propagation measurements for extremely high frequency (EHF) or millimeter wave (mmW) applications. For that specific application, there is much less tolerance for position error (under a meter). Further, delivering a position measurement with an accuracy that is close to that claimed by the GNSS receiver manufacturer (e.g.  $\pm(15 \text{ mm} + 1 \text{ ppm})$  RMS in the vertical plane) [2] will allow us to better investigate the effects of knife-edge diffraction from buildings and deliver more accurate analysis in general.

#### IV. DRIVE TEST RESULTS AND ERROR ANALYSIS

Field testing of the precision geolocation system has progressed from benchtop setup and integration to static, outdoor testing in the drive test vehicle to data collection during a clutter measurement campaign. In this section, excerpts from the final two testing cases will be discussed. Field testing began with logging sensor data (GNSS and IMU) during a clutter measurement campaign in March of 2017 and continued through June of 2018, ending with an initial, full system test in downtown Denver. Dynamic field testing for the final iteration of the precision geolocation system prior to launch will be completed by the beginning of autumn 2019. A subsequent report on the final system and test results will be delivered afterwards.

##### A. Static Testing

Fig. 3 and Fig. 4 below provide a good synopsis of the progress that has been achieved so far in the project under challenging, real-world, static test conditions.

The two left-hand images in Fig. 3 show the position of the drive test vehicle within an alleyway that occluded approximately 25% of the visible sky. The right-hand image shows a positional drift comparison between: 1. a spectrum analyzer with "hockey puck" antenna and GPS receiver option (green track), and 2. the Trimble GNSS receiver without correction sources (blue track); positional drift is approximately 100 ft. and 125 ft., respectively.



Fig. 3. A set of images illustrating typical static, urban test canyon conditions in downtown Boulder, CO.

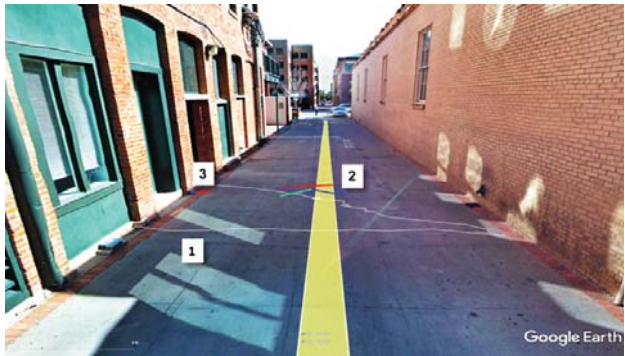


Fig. 4. This image illustrates the effectiveness of corrections and the refinement of our position estimates over time; drift error decreased from approximately half a block to less than 12 inches.

In Fig. 4, the KML track at position 1 (white) is a different view of the spectrum analyzer generated track shown in Fig.3; drift is approximately 100 ft. Position 2 shows a KML track after SBAS and RTX corrections had been activated on the GNSS receiver; drift is approximately 2.5 ft. The small track near 3 shows the best positional drift achieved to date; the GNSS receiver is using SBAS, RTX, and RTX and the total drift, or the extent of position variance is under 1 ft.

At the start of the project, ITS engineers spent a lot of time trying to optimize the Trimble GNSS receiver so that it produced results that approached the manufacturer's specifications [2]. The results shown above were collected before the end of November 2017.

One method of arriving at the optimal settings while under static, "blue sky" conditions was to place the drive test vehicle near a known, National Geodetic Survey (NGS) survey benchmark.

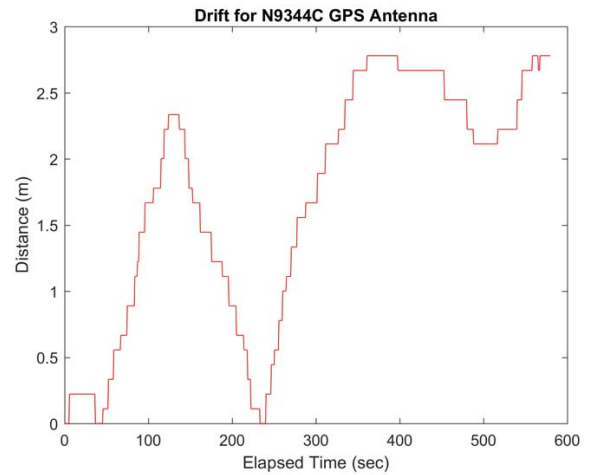


Fig. 5. A plot of positional drift in the horizontal plane vs. elapsed time for a handheld spectrum analyzer with GPS options and "hockey puck" antenna set up near NGS Benchmark LL1143.

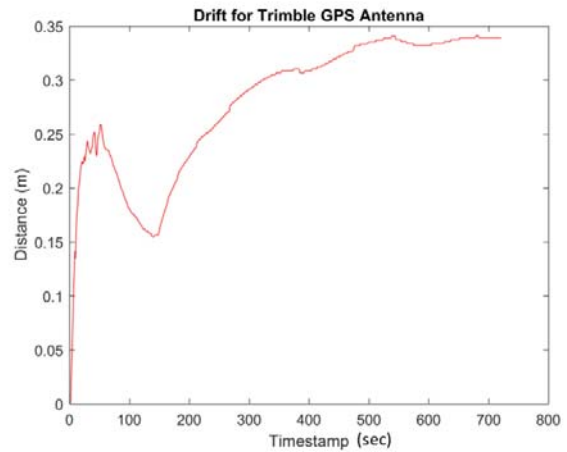


Fig. 6. A plot of positional drift in the horizontal plane vs. elapsed time for a Trimble BX982 GNSS receiver and Zephyr Geodetic 2 position antenna set up near National Geodetic Survey (NGS) Benchmark LL1143.

The results shown in Fig. 5 and Fig. 6 clearly demonstrate a dramatic increase in horizontal, positional accuracy simply by using a high-quality, optimized GNSS receiver. The total positional drift variance in Fig. 5 decreases after a six-minute settling period to approximately half a meter. In Fig. 6, the total positional drift eventually settles to approximately 0.34 m away from our initial guess (at Distance = 0) and the variance seems to reach a minimum after an eight-minute settling period. The lowest figure for the standard deviation of longitude error achieved to date under static, "blue sky" conditions after a settling period is 5 mm, which is approximately equal to the manufacturer's specification for RTK positioning accuracy in the horizontal plane [2].

### B. Dynamic Testing

Field testing with a moving test vehicle proceeded in a similar manner to the static case in that short-duration drive tests were conducted where there was no clutter in the first Fresnel

zone between the transmitter (medium Earth Orbit GNSS constellations) and the receiver as well as no occlusions to the southwest of the drive test vehicle.

After establishing a good level of positional consistency under static conditions, an attempt was made to verify the precision of the system while driving. Fig. 7 shows the drive test location for this initial, dynamic test.

Three loops consisting of two counterclockwise circuits were completed for the test. The Loop 1 test began and ended at marker 1, while Loops 2 and 3 began/ended at marker 2. It is difficult to discern the individual tracks of the three loops even in a large, high quality photo. This is mainly because the tracks are very similar and overlap each other. A close-up view of the tracks is shown in Fig. 8.

Fig. 8 demonstrates a good level of precision over three separate drive tests. There is some small variation between the three tracks when passing through the corner, but that is more likely due to driver error and a smaller number of data points collected during Loop 2, resulting in a less smooth track. On the portions of the road that are relatively straight, there appears to be little variation: the position antenna is clearly attached over the passenger side of the drive test vehicle and there are no large variations in the track due to strong multipath conditions.



Fig. 7. A Google Earth image showing three, separate KML tracks captured by the precision geolocation system on March 21, 2018.

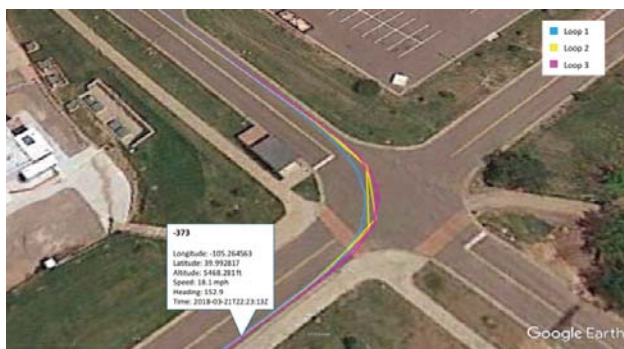


Fig. 8. A zoomed-in view of the three Google Earth KML tracks shown above in Fig. 7. KML parameters for point 373 are shown for illustrative purposes.

### C. Analysis of a Typical Position Estimate Error

Having achieved a satisfactory level of precision while collecting position data while moving, the team readied itself for

the next clutter measurement opportunity. Clutter measurement testing was conducted throughout the Salt Lake City area during the latter half of June 2018 in areas with relatively uniform propagation characteristics, e.g. dense urban, light industrial, suburban, and rural.

The system performed as expected in that the final position estimate in the precision geolocation system's KML track file generally agreed closely with the KML track file of the drive test route — with one exception: dense urban canyons. Fig. 9 shows an example of significant positional drift encountered while driving the test vehicle through one of Salt Lake City's urban canyons. At this point, the drive test vehicle, which proceeded from right to left in the figure, was stopped for a short time while waiting for a traffic light to change.

After returning from the field, an attempt was made to explain the reason for the anomalous drift. Fig. 10 and Fig. 11 below show unfavorable conditions for both the number of satellite vehicles (SV) and positional dilution of precision (PDOP), a measure of the confidence of position estimates; a higher PDOP value indicates poor satellite geometry.

The building near marker 1 in Fig. 9 below (111 Main) is the third tallest building in Salt Lake City at 23 stories [9]. At this height, nearly 90 degrees of southwest view of the sky is obscured. At position 1 in Fig. 10 below, we see a sudden drop in the number of satellite vehicles seen by the GNSS position antenna. Another drop is seen to the left of position 2 after the intersection, though the minimum number of satellite vehicles for three-dimensional positioning is present (four are needed, five were observed).



Fig. 9. A Google Earth image of a KML track generated by the precision geolocation system.



Fig. 10. A heat map overlay showing the number of satellite vehicles in view while drive testing on a satellite image of the area under analysis, i.e. significant positional drift at position 2.



Fig. 11. A heat map overlay showing Positional Dillution of Precision (PDOP) values encountered while drive testing on a satellite image of the area under analysis, i.e. significant positional drift at position 2.

## V. CONCLUSION

This paper presented a summary of the work that ITS has undertaken over the past two years in precision geolocation. At the start of the project, geolocation information was rarely used at ITS due to the large amount of error. Since then, and because of the improvements made in horizontal position estimation, geolocation has begun to be considered more seriously within the context of RF propagation measurements in the field.

A description of the four types of equipment in the system (signal sources, sensors, correction sources, and processing) was provided as well as the capabilities and interfaces between each piece of equipment. The most important equipment-related takeaway is that a properly-configured GNSS receiver has the highest impact on positional accuracy and precision. Additional sensors (LiDAR and wheel shaft encoders) may be added to the system later, but these, along with the IMU and visual odometry sensors, will only augment the position estimate provided by the GNSS receiver and mitigate “free run” estimates when in urban canyons.

Next, the implications of positional error were discussed. For an AWS-3 signal, the margin of error for positional drift in the horizontal plane is approximately 11.5 m, and the need for

tighter error tolerances for mmW measurements was raised. A project goal to achieve a similar level of accuracy as specified by the manufacturer was attained.

A subset of testing results under static and dynamic conditions, as well as an example of error analysis was presented. To date, the project has achieved a dramatic decrease in positional accuracy under static conditions (~30 m to 5 cm), and demonstrated that a relatively small investment in a quality GNSS receiver yields much better results than a spectrum analyzer and “hockey puck” antenna. We found that the precision geolocation system performed very well in rural, suburban, and light industrial geographies, but that there is still room for improvement when conducting measurements in urban canyons.

The project is still active, though it should be completed within the current fiscal year. The goals for the current year are to finish sensor data fusion in software, document the system, and begin using it full-time during measurement campaigns.

## ACKNOWLEDGMENT

The author wishes to thank the entire clutter measurement team, especially Ms. Chriss Hammerschmidt and Dr. Robert Johnk for their continued guidance and technical expertise. The author would also like to thank Dr. Keith Gremban and Mr. Eric Nelson for funding this research.

## REFERENCES

- [1] A. E. Paulson, “ISART Workshop on Best Measurement Practices Precision Geolocation,” in ISART 2018 • Path Lost: Navigating propagation challenges for ultra-dense wireless systems, Boulder, 2018. [[https://www.its.blrdoc.gov/media/66504/paulson\\_isart2018.pdf](https://www.its.blrdoc.gov/media/66504/paulson_isart2018.pdf)].
- [2] Trimble Navigation Limited, “Trimble BD982 GNSS Receiver Module,” Trimble Navigation Limited, Sunnyvale, 2014.
- [3] Intuicom, Inc., “Intuicom® Wireless RTK Bridge - Cellular User Guide,” Intuicom, Inc., Boulder, 2009.
- [4] UNAVCO, “Real-Time GPS Data,” UNAVCO, 16 August 2017. [Online]. Available: <https://www.unavco.org/data/gps-gnss/real-time/real-time.html>. [Accessed 6 March 2019].
- [5] I. Henne and P. Thorvaldsen, Planning Line-of-Sight Radio Relay Systems, Second ed., Bergen: NERA Telecommunications, Ltd., 2002, p. 194.
- [6] Federal Communications Commission, “Advanced Wireless Services (AWS),” Federal Communications Commission, 13 April 2017. [Online]. Available: <https://www.fcc.gov/wireless/bureau-divisions/broadband-division/advanced-wireless-services-aws>. [Accessed 7 March 2019].
- [7] National Association of City Transportation Officials, Urban Street Design Guide. [Accessed 10 April 2019].
- [8] C. A. Hammerschmidt and R. Johnk, “Extracting Clutter Metrics From Mobile Propagation Measurements in the 1755-1780 MHz Band,” in IEEE Military Communications Conference, Baltimore, 2016. [<https://www.its.blrdoc.gov/publications/3166.aspx>].
- [9] Emporis GmbH, “111 Main,” Emporis GmbH, 7 March 2019. [Online]. Available: <https://www.emporis.com/buildings/1211453/111-main-salt-lake-city-ut-usa>. [Accessed 7 March 2019].